Variable Entrained Flow Ejector

Egoi Ortego Sampedro

Variable Entrained Flow Ejector

Egoi ORTEGO SAMPEDRO

Mines ParisTech, Centre d'Efficacité Energétique des Systèmes, Palaiseau, France

egoi.ortego@mines-paristech.fr

ABSTRACT

In refrigeration systems ejectors are used to increase the pressure of an entrained or secondary stream using the energy of a high pressure and high temperature primary stream. The lack of flexibility of ejectors contributes to their modest deployment in the refrigeration market and more widely in industry. In general, for gas-gas ejectors, the highest ejector performance is obtained at the critical pressure ratio. For lower pressure ratios the entrainment ratio remains constant, and for higher pressure ratios it drops rapidly to zero. This behavior makes the load control hard to handle. In order to increase the flexibility of ejectors and also the average entrainment ratio, variable geometry solutions exist. Those solutions allow the variation of the primary stream nozzle throat section or the nozzle axial position. With those solutions the secondary mass flow remains limited to a maximum fixed by the mixing chamber diameter. In this paper, a new variable geometry ejector concept is explored that allows increasing the secondary stream flow rate as the discharge pressure decreases. The ejector performance is estimated by computational fluid mechanics. This is compared to a geometry from literature. The case study is an R134a ejector driven refrigeration cycle using waste heat. The interest of the new variable geometry ejector on the seasonal Energy Efficiency Ratio is analyzed.

1. INTRODUCTION

The advantage of using ejectors in refrigeration cycles is nowadays well established. Either they allow the recovery of throttling expansion energy in a simple and economical way for example in compressor driven transcritical CO_2 cycles (Banasiak, et al., 2015), or may run cycles powered by waste heat (Valle, et al., 2014) as the one presented in Figure 1.

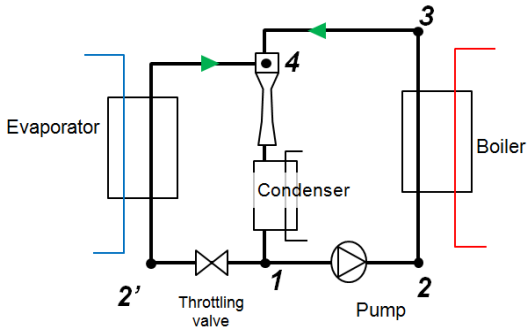

Figure 1 : waste heat driven refrigeration ejector cycle

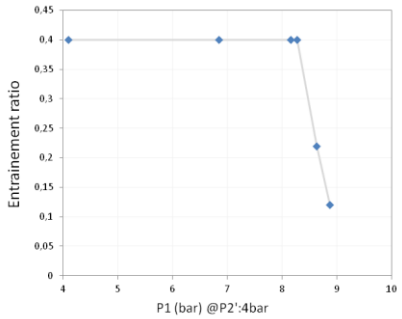

Figure 2 : ejector entrainment ratio example from (Valle, et al., 2014)

The main drawback of ejectors is their strong sensitivity to operating conditions and the subsequent lack of flexibility. Indeed ejector design often requires a compromise between the compression ratio ($P_1/P_{2'}$) and the entrainment ratio ($\mu = m_{2'}/m_2$) especially when dealing with refrigeration cycles condensing just above ambient temperature.

The effect of the mixing chamber cross section on the ejector performance was explored by Jia Yan (Jia & Wenjian, 2012). In this experimental work, various mixing chambers with different diameters were tested separately. It can be read in the cited work how the mixing chamber's diameter (Dm) affects the ejector's behavior; the critical point (or stall point) is particularly sensitive to this diameter. When Dm is reduced, the maximal compression ratio increases and maximal entrainment ratio decreases, when Dm increases, the inverse is observed. The compromise between these two variables must be made by taking into account the climatic conditions in which the system will work. Once the design Dm has been chosen, the behavior of an ejector looks like illustrated in Figure 2. It shows how beyond the critical point, the entrainment rate is greatly degraded and how below the critical point it is constant. This behavior is due to choked supersonic flow accompanied by a shock wave in the mixing chamber. The maximum speed reached in the mixing chamber being only a function of the upstream conditions, at constant mixing diameter, the entrained flow rate will be identical for compression ratios below the critical. When the outlet pressure is increased, a displacement of the shock wave towards the primary nozzle is observed, and finally the shock wave vanishes as the critical point is passed giving

way to the entrained flow reduction and then inversion. When comparing this behavior to the ideal behavior we find that the observed performance is the closest to the theoretical performance only at the critical point where the ejector efficiency is the highest (Valle, et al., 2014).

Variable geometry solutions have been widely studied for ejectors. Literature provides several examples of variation of primary throat cross section by movable spindles (Varga, et al., 2013) (Liu, et al., 2012) (Gullo, et al., 2020), as well as solutions for the axial gap variation between the primary outlet and the mixing chamber. The former kinds of solutions help in reducing the primary flow rate in order to reduce the energy consumption at the boiler in a heat driven chiller (such as the one presented in Figure 1). This system has two main drawbacks, the first being that the secondary flow rate, and thus the cooling power is constant for all condenser pressures below the critical points. The second, if using a centrifugal pump to drive the working fluid, is that a change on primary flow rate at the same boiler pressure implies a drop in pumping efficiency. The second solution seems to have a limited interest according to the experimental sensibility analysis presented in (Valle, et al., 2014); indeed it seems that an optimal axial position exists for all the pressure range. So since the optimum doesn't depend on outlet pressure, no adaptation control can be done by this solution (at least at given inlet conditions).

A new concept of variable geometry ejector is proposed in this article. It is evaluated by CFD simulations. After discussing the entrainment ratio results, a brief flow analysis is given and finally the seasonal Energy Efficiency Ratio (EER) is computed with weather data from the Paris area in France.

2. Geometry

We propose here a solution for a geometry variation of the mixing chamber and diffuser. It consists mainly of the division of the initially cylindrical ejector's outer body in two parts by an axial symmetry plane; one of the parts is then laterally displaced; the basic idea is presented in Figure 3. The aim is to be able to vary the mixing chamber cross section. This solution allows operating at a multitude of equivalent mixing chamber cross sections while this is a fixed feature in conventional ejectors. The optimal opening will depend on the actual discharge pressure defined by the condensing temperature related to the outdoor temperature. If the last is low, the opening can be increased since the required critical pressure is lower, and if the temperature is higher, the opening would be reduced in order to increase the critical pressure. Such a variable mixing chamber would allow maximizing the entrained flow for each condensing temperature by adapting the stall point to outdoor conditions..

The main technical difficulty to be addressed is the sealing between the two parts. Ejectors are elongated so an oblong sealing solution was imagined. Such a concept is presented in Figure 3.

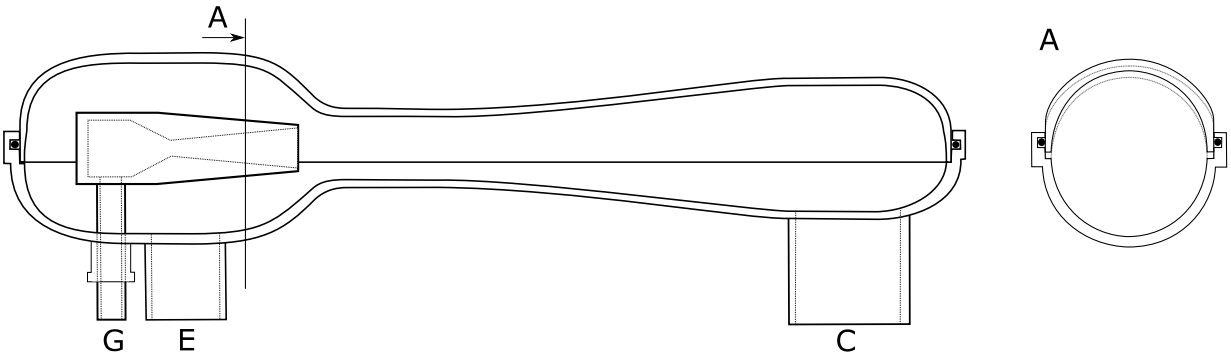

Figure 3 : a variable geometry ejector concept

The use of such a sealing solution requires a lateral flow outlet; this flow deviation was not modeled in here since it is not symmetric in the central plane perpendicular to the side view of Figure 3 and it would require supplementary computational effort. Instead the pressure drop generated by such a deviation was estimated to be lower than 1% of the outlet pressure ($\Delta P = f/2\ \rho\ V^2$, with f=1.1(IDEL'CIK, 1969) and V=18m/s).

As a first step in the performance characterization of such an ejector, a modification applied to a reference literature ejector was evaluated by CFD simulations. The reference ejector is a gas-gas R134a ejector design for a waste heat driven refrigeration cycle and the original performance measurement and geometry are presented in (Jia & Wenjian, 2012). The original geometry is presented in the Figure 4 a) and the modified geometry cross section view in Figure 4 b); these figure show cross sections of the computational domain; two symmetry planes were used to reduce the 3D computational domain volume (see S1 and S2 in Figure 4 b)). In Figure 4 b) the opening is presented; the primary nozzle was maintained centered on initial reference position.

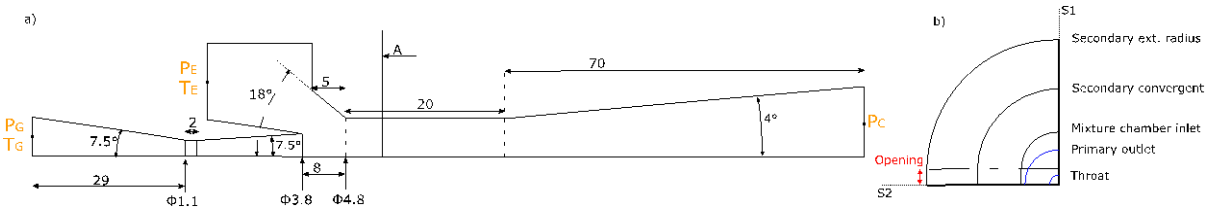

Figure 4 : a) base geometry from (Jia & Wenjian, 2012), b) cross section view of the modified geometry at axial position A

Various opening values were simulated to characterize the entire compression ratio range. Only one set of inlet conditions was explored in this preliminary work: P_G 25bar, T_G 78°C, P_E 4.14bar, T_E 11°C. Various outlet pressures P_C were tested representing various condensing temperatures (T_{cond}); for condensation temperatures ranging from 10°C to 32°C, condensing temperature ranges from 4bar to 8bar. If pressure losses are neglected in the heat exchangers, the compression ratio P_1/P_2, equals P_C/P_E.

3. Numerical methods

The presented numerical simulations were performed using the commercial code Ansys CFX. The flow was assumed to be steady, compressible and turbulent. The Peng-Robinson equation of state was used for R134a; this EOS is described as sufficiently accurate by different authors for HFC gases (Mazzelli & Milazzo, 2015)(Brown, 2007). The kwSST turbulence was used as recommended in literature (Mazzelli & Milazzo, 2015). As boundary conditions, static pressures were set at the inlets and the outlet, and the inlet gas temperatures were also set. The wall was modeled as adiabatic. The CFX solver is a coupled solver using a pseudo-transient formulation. A bounded second-order upwind scheme was selected for the discretization of the convective terms. A steady state simulation was done. The physical time step was set to 4.10^{-6} s. The simulations were supposed to be converged when all the residuals were lower than $10.^{-5}$ and the mass balance was lower than 1%.

The mesh was built following the recommendation from literature (S.Croquer, et al., 2016) for such supersonic ejectors; the main volume was meshed using tetrahedral elements and hexahedral elements were used close to the wall. The mesh was generated using Ansys Workbench standard meshing software. A mesh sensitivity analysis was conducted; the results on primary and entrained flow rates are presented in Table 1; the figures give the relative difference to the finest grid results. Finally a maximum mesh size of 8e-4m and parietal first layer thickness of 1.5e-4m were adopted.

Table 1 : grid convergence; mass flow rate variations;

Number of nodes		5,9E+04	1,6E+05	2,5E+05	4,2E+05
Difference to the finest	Primary	-2,1%	-0,7%	0,1%	0,0%
	Entrained	3,3%	1,4%	-0,1%	0,0%

4. Simulation results

4.1. Entrainment ratio

Three opening positions were explored (0mm, 0.7mm, 1.1mm) covering the total outlet pressure range for operating conditions of the reference case (down to 10°C of condensing temperature). A series of simulations was done for each position. The reference ejector's experimental entrainment values and the results of the CFD simulation are presented in Figure 5.

The simulation's entrainment ratio for the reference case is over estimated by around 10% at critical pressure. The critical pressure is relatively well predicted. The computed primary flow rate was 39g/s; it was the same for all cases.

The critical points for the two other positions show increasing entrainment ratio and deceasing critical pressure (corresponding to lower condensation temperatures) when increasing opening. That shows how when the ambient temperature decreases, the proposed ejector concept allows increasing substantially the entrainment ratio. The global behavior of such an ejector can be modeled by the line connecting the critical points at different opening positions. In the section dealing with the annual refrigeration performance, the simulated values will be reduced to take into account the over-estimation of the entrainment ratio by the CFD simulations. The "90%" grey line on Figure 5 will be used as model.

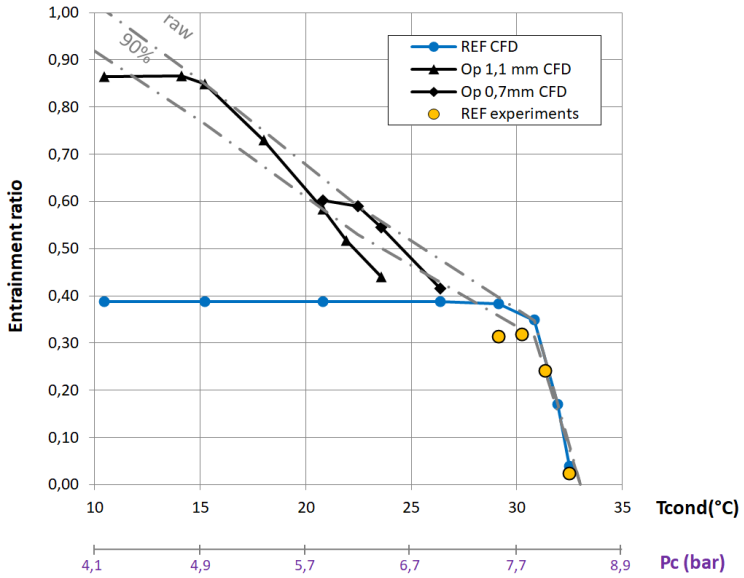

Figure 5 : entrainment ratio; references and simulations for P_E = 4.14bar

Regarding the largest opening situation, it is remarkable, for pressures above critical, how the entrainment ratio reduction rate is lower than for the original simulated and measured data. An analysis for this behavior is proposed in the next section.

4.2. Flow situation in the modified ejector

A brief analysis of the flow in the ejector is presented in the following section.

The Mach number contours are provided in Figure 6 for the reference and ‘’1.1mm’’ geometries critical points (7.5bar and 4.6bar outlet pressures respectively). For the same geometries, a case at higher pressure is presented, 8bar and 6.5bar respectively. These figures show the views of the both symmetry planes reported in the same plane.

Figure 6 : Mach number plots for various cases

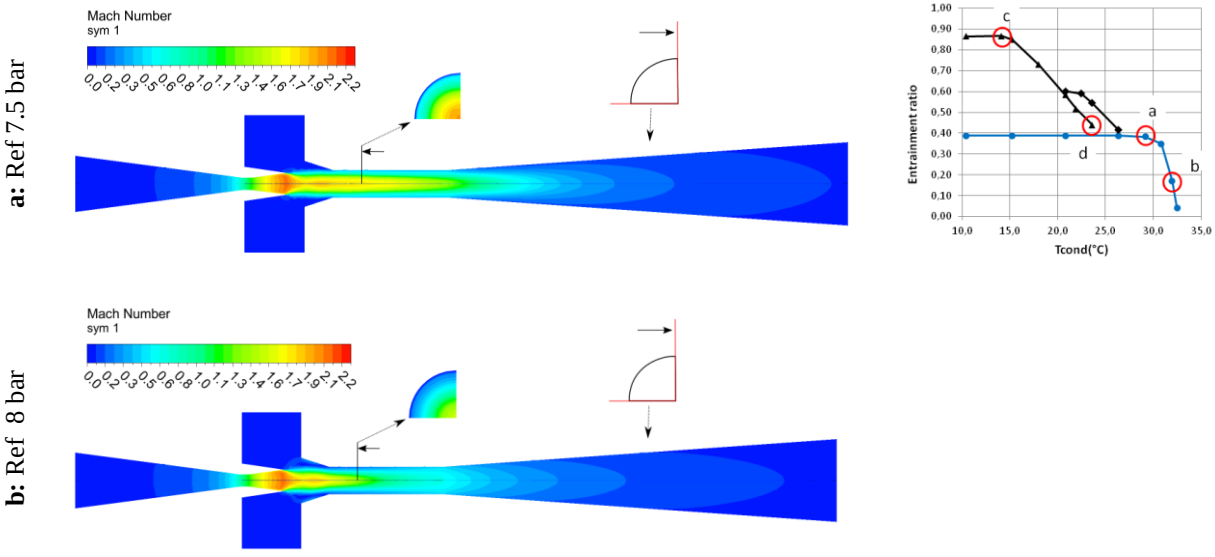

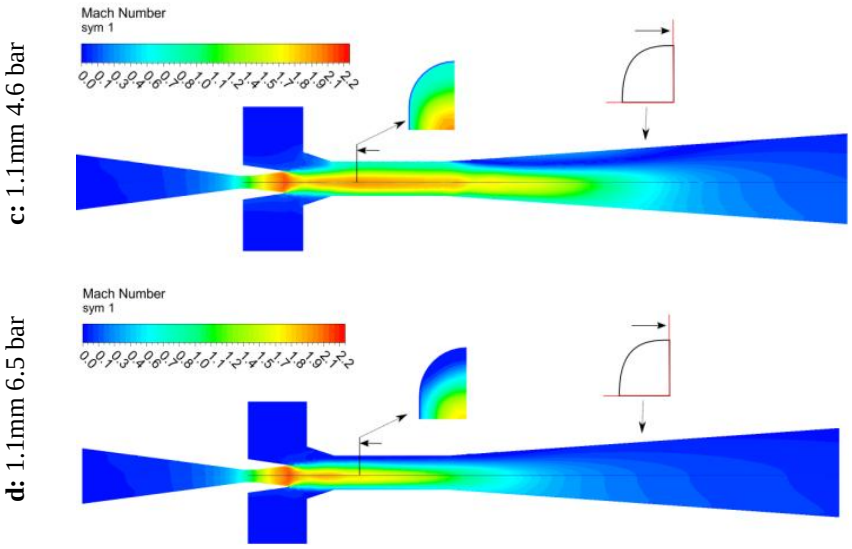

The behavior at overcritical pressures is rather different for the two ejector openings. In the first case the entrainment ratio reduction is fast; this is accompanied by an important reduction of the volume occupied by the supersonic gas (see "a" and "b" cases in Figure 6). For 1.1mm opening (cases "c" and "d"), at the highest pressure ("d"), the high velocity area remains relatively large; it seems to be due to a flow attachment to the wall closest to the axis (the direction transverse to the opening direction). This attachment is affected when increasing condensation pressure and thus the entrainment ratio would be lower than the critical entrainment ratio of the reference geometry. Besides, at the lowest pressure, a supersonic velocity flow occupies all the mixture chamber cross section (case "c") leading to a very high entrainment ratio.

4.3. Cooling cycle efficiency

The temperature dependent efficiency ($EER_T(T)$) was estimated by a simple refrigeration cycle model. The cycle is shown in Figure 7 and it corresponds to system presented by Figure 1.

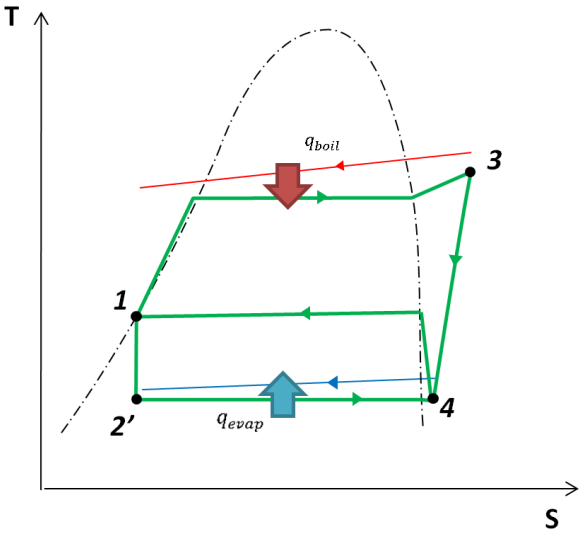

Figure 7 : refrigeration cycle

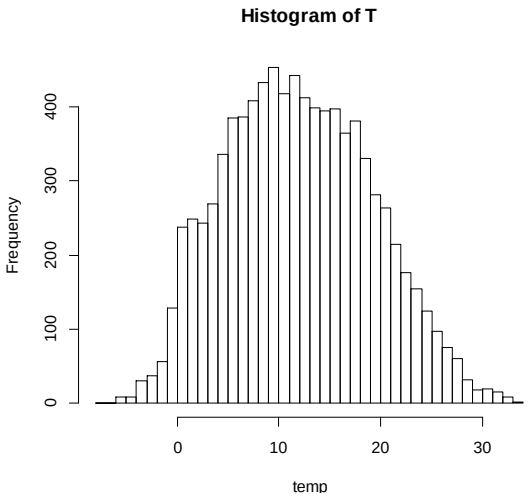

Figure 8 : Orly station outdoor temperatures frequencies histogram ; class width 1K

The cycle refrigeration efficiency is described by equation (1).

$$EER_T(T) = \mu(T_{cond})\frac{\Delta h_{evap}}{\Delta h_{boiler}} \quad (1)$$

The boiler inlet enthalpy is supposed to be equal to the condenser outlet enthalpy (pump Δh neglected) and the outlet enthalpy is computed from the ejector primary stream inlet conditions. The evaporator inlet enthalpy is supposed to be equal to the condenser outlet enthalpy and the saturated gas enthalpy is used for the evaporator

outlet. No pressure losses are considered in the heat exchangers. Operating conditions are the following: boiler pressure is P_G, boiler outlet temperature is T_G, evaporator pressure is P_E and evaporator outlet is at unit vapor quality. These assumptions are expressed in equations (2) and (3). The condenser temperature (T_{cond}) will be supposed higher than the ambient temperature ($T_{cond} = T + pinch$; 3K ≤ pinch ≤ 5K).

$$\Delta h_{boiler} = h_3(P_G, T_G) - h_1(T_{cond}, x = 0) \quad (2)$$

$$\Delta h_{evap} = h_4(P_E, x = 1) - h_2,(T_{cond}, x = 0) \quad (3)$$

The entrainment ratio is modeled here by the gray lines in Figure 5. Since the CFD results overestimated the reference experimental data, a 90% correction factor is applied to the modified ejector raw CFD results.

The seasonal efficiency (EER_s) computed here is based on annual energy exchanged in the evaporator compared to the one used on the boiler. The boiler energy is computed by the temperature dependent efficiency ($EER_T(T)$). And the required cooling energy is computed by a required cooling power model ($Pu_{cool}(T)$) and the temperature frequency ($Nh(T)$ in number of hours per year) for a given location.

$$EER_s = \frac{E_{cool}}{E_{hot}} = \frac{\sum[Pu_{cool}(T)\, Nh(T)]}{\sum[Pu_{cool}(T)/EER_T(T)\, Nh(T)]} \quad (4)$$

The cooling load model helps in attributing to each temperature a weight depending on power-temperature profile. The used cooling load model was the one presented in (Tsimpoukis, et al., 2020) for a supermarket store. Ambient temperature (T) is in degree Celsius. It doesn't include dehumidification load.

$$Pu_{col}(T)[kW] = \max(0kW, 11.8\,(T - T_{ref})) \quad (5)$$

The lower clipping to 0kW avoids negative values. The reference temperature (T_{ref}) was 20°C in the cited paper; it could change depending on the application (data center, fresh food storage...). No efficiency penalty was adopted here when the entrainment ratio values were too low (for highest temperatures for example). Part load operation effects on efficiency were not modeled in this preliminary work.

The ambient temperature frequencies were obtained using the hourly averaged Energy Plus weather data based on the Orly station measurements from 2004 to 2018. The temperatures frequencies histogram is shown in Figure 8.

The computed temperature dependent efficiencies ($EER_T(T)$) for both reference and modified ejectors are shown in Figure 9. The condensing temperature does not affect the reference case efficiency significantly, mainly because the entrainment ratio is constant over the treated pressure range. The modified ejector shows an increasing efficiency when decreasing the condensing temperature.

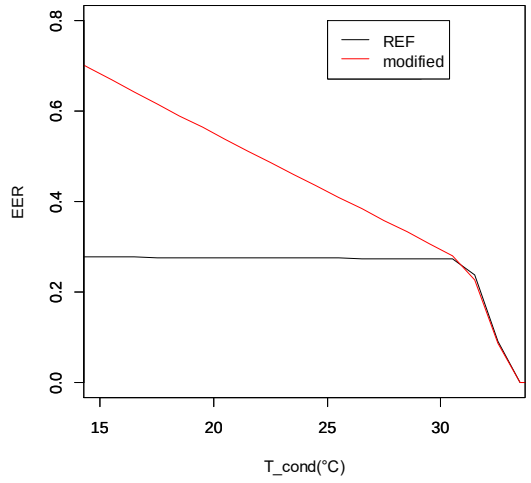

Figure 9 : $EER_T(T)$ of the reference and modified ejectors

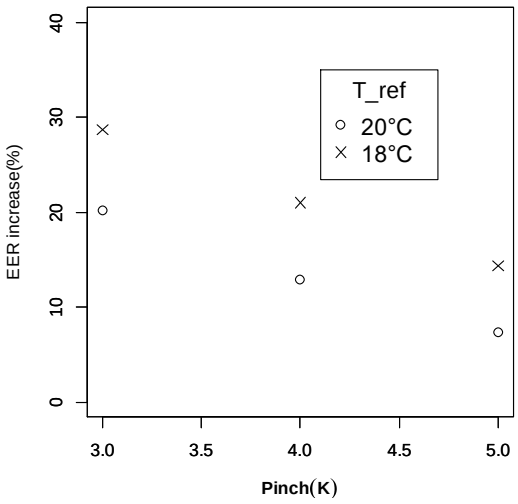

Figure 10 : relative $EER_T(T)$ difference

The relative seasonal efficiency increase possible with the modified ejector was calculated for various cases: two reference temperatures were used for the cooling load estimation for various pinch values. The results are shown in Figure 10. The lower the reference temperature the higher the improvement potential; this is due to the higher entrainment ratio at lower temperatures causing the increase of the average efficiency. The reduction of the pinch, increases the improvement potential because it causes a condensing pressure reduction and thus a shift on the entrainment ratio data towards higher ambient temperature values.

The improvement potential is strongly affected by the initial ejector design and it's adaptation to a given weather situation. Higher temperature variation over a year provides more opportunity for improvement by an adaptable geometry. The presented analysis should be completed with supplementary weather data and other initial ejector designs in order to go further in the investigation of the potential offered by this new ejector concept.

5. Conclusion

This paper presents a lateral geometry variation ejector concept. The proposed solution allows increasing the mixing chamber cross-sectional area leading to an entrained flow increase at sub-critical outlet pressures. The performance investigation was based on a reference gas-gas R134a ejector geometry from literature to which the lateral opening concept was applied. CFD simulations were done with three opening positions and several pressures leading to a complete characterization of the device. An analysis of the flow is also proposed were the gas Mach number plots are discussed.

Subsequently, the entrainment ratio data were used to estimate the benefit this kind of ejector could bring to the seasonal efficiency of a boiler driven refrigeration cycle. The improvement potential depends on the pinch temperature difference at the condenser and the reference temperature of the cooling demand profile. As an example, for a 4K pinch and 18°C reference temperature the seasonal EER increase was 21%.

Further investigation needs to be done especially to develop a design strategy of such an ejector depending on the weather data. Besides, an experimental validation of the concept is necessary. Beside a deeper analysis of non axisymmetric supersonic flows could help to improve the design methods for such ejectors.

6. NOMENCLATURE

Roman characters

E	energy [J]
h	enthalpy [J kg^{-1}]
N_h	number of hours
P	absolute pressure [bar]
P	absolute pressure [bar]
Pu	power [W]
T	temperature [K]
q	heat flow [W]
x	quality

Greek characters

Δ	difference
μ	entrainment ratio

Indexes

C	Outlet
E	Entrainment
G	Primary
S	Seasonal
T	Temperature dependent

Acronyms

EER	Energy Efficiency Ratio

7. References

Anon., 2014. Experimental results with a variable geometry ejector using R600a as working fluid. *International Journal of Refrigeration,* Volume 46, pp. 77-85.

Ansys, 2014. *Ansys V16 Users Guide.* s.l.:s.n.

Banasiak, K. et al., 2015. Development and performance mapping of a multi-ejector expansion work recovery pack for R744 vapour compression units. *International Journal of Refrigeration,* Volume 57, pp. 265-276.

Brown, J. S., 2007. Predicting performance of refrigerants using the Peng–Robinson Equation of State. *International Journal of Refrigeration,* pp. 1319-1328.

Chen, J., Havtun, H. & Palm, B., 2014. Investigation of ejectors in refrigeration system: Optimum performance evaluation and ejector area ratios perspectives. *Applied Thermal Engineering,* pp. 182-191.

Elbel, S. & Lawrence, N., 2016. Review of recent developments in advanced ejector technology. *International Journal of Refrigeration,* Volume 62, pp. 1-18.

Gullo, P. et al., 2020. A review on current status of capacity control techniques for two-phase ejectors. *International Journal of Refrigeration,* Volume 119, pp. 64-79.

IDEL'CIK, I., 1969. *Memento des pertes de charge. Chp.VI.* s.l.:Eyrolles.

Jia, Y. & Wenjian, C., 2012. Area ratio effects to the performance of air-cooled ejector refrigeration cycle with R134a refrigerant. *Energy Conversion and Management,* Volume 53, pp. 240-246.

Liu, F., A.Groll, E. & Li, D., 2012. Investigation on performance of variable geometry ejectors for CO2 refrigeration cycles. *Energy,* Volume 45, pp. 829-839.

Mazzelli, F. & Milazzo, A., 2015. Performance analysis of a supersonic ejector cycleworking with R245fa. *International Journal Of Refrigeration,* pp. 79-92.

S.Croquer, S.Poncet & Z.Aidoun, 2016. Turbulence modeling of a single-phase R134a supersonic ejector. Part 1: Numerical benchmark. *International Journal of Refrigeration,* pp. 140-152.

Tsimpoukis, D. et al., 2020. Energy and environmental investigation of R744 all-in-one configurations for refrigeration and heating/air conditioning needs of a supermarket. *Journal of Cleaner Production,* Volume 279.

Valle, J. G. d., Jabardo, J. S., Ruiz, F. C. & Alonso, J. S. J., 2014. An experimental investigation of a R-134a ejector refrigeration system. *International journal of refrigeration,* Volume 46, pp. 105-113.

Varga, S., Lebre, P. M. & Oliveira, A. C., 2013. CFD study of a variable area ratio ejector using R600a and R152a refrigerants. *International Journal of Refrigeration,* Volume 36, pp. 157-165.